ISSN 2616-5880 Vol. 5, Issue 3: 79-84, DOI: 10.25236/AJMC.2024.050312

A plasma resonance-based broadband metamaterial absorber design

Yi Cao[1,a,*], Xuanjun He[1,b]

[1]*College of Physics and Optoelectronic Engineering, Shenzhen University, Shenzhen, China*
[a]*2021270062@email.szu.edu.cn,* [b]*2021270249@email.szu.edu.cn*
[*]*Corresponding author*

Abstract: *The perfect absorber is one of the most important applications in metamaterials technology, which has received much attention based on its ultrathin characteristics and design flexibility, but also suffers from the disadvantage of narrow absorption bandwidth. Therefore, this paper proposes a broadband metamaterial perfect absorber based on a metal-dielectric-metal structure, and its absorption mechanism and physical principle are analyzed. The results show that the metamaterial absorber realizes perfect absorption from visible to near-infrared wavelength. In addition, this study investigated and compared the effects of various materials and geometrical structures on the absorption performance, and analyzed the absorption spectra about different polarized directions and large-angle oblique incident light. The designed absorber with its simple structure and broad absorption spectrum is expected to be widely used in various industries, like solar cells, infrared imaging, and detectors.*

Keywords: *Metamaterial Absorber, Near infrared spectrum, Plasmonic, FDTD*

1. Introduction

Electromagnetic metamaterials represent a category of synthetic materials that exhibit sub-wavelength periodicity. Their distinctive optical characteristics are attributed to the meticulously crafted artificial periodic structure, which endows them with exceptional physical properties and enables them to excel in the collection, transmission, and modulation of electromagnetic waves in ways that natural materials are unable to match. Consequently, they are employed extensively in several applications, including stealth technology [1], negative refractive index [2], wave absorbers [3,4], and modulators. Among these, metamaterial absorbers offer the advantages of a simple structure and high wave absorption efficiency. This technology has been employed in several fields, including spectrum imaging, sensors, and energy harvesting, and has emerged as an effective solution to electromagnetic interference.

As research progresses, the bandwidth of electromagnetic metamaterial absorbers has gained significant attention within the scientific community. Due to the resonant nature of electromagnetic metamaterial absorbers, their absorption is closely related to frequency and structure. The majority of existing structures exhibit narrow-band absorption. To date, scientists and researchers concentrate on using the combination of multi-size unit structures to expand the bandwidth. However, the resulting bandwidth remains inadequate, and the multi-size patterning structure increases the complexity and difficulty of the preparation process and leads to higher costs and difficulties in universal access. Therefore, it is necessary to develop an absorber with ultra-wideband and high absorption capabilities in simple structural designs, which is an area of focus within academic research.

This paper presents the design of a cylindrical absorber based on the phenomena of propagating surface-isolated primitive resonance (PSPR) and localized surface-isolated exciton resonance (LSPR) in electromagnetic metamaterials. The absorber is composed of three distinct layers. In this work, the finite-difference time-domain (FDTD) method is used for simulation modeling to study the absorption characteristics and field distribution. The proposed absorber is well suited for applications in solar photovoltaics, optical communications, microwave [5,6], and so forth, as it has extremely high absorption ability.

2. Design of structure

The structural parameters of this metamaterial absorber can be analyzed using the equivalent medium

ISSN 2616-5880 Vol. 5, Issue 3: 79-84, DOI: 10.25236/AJMC.2024.050312

theory [7,8] when studying its interaction with incident light because its size is smaller than the operating wavelength. In the context of the equivalent medium theory, the metamaterial absorber is regarded as a homogeneous material, and its characteristics are delineated through the S-parameter inversion method. As shown in Figure 1, the absorber is composed of three metamaterial layers, arranged from top to bottom as Ti, SiO_2, and Al. The Al layer serves as the substrate, with a thickness exceeding its skinning depth, which enables nearly total reflection of incident light. SiO_2 and Ti layers primarily contribute to the absorptivity as the absorbing elements.

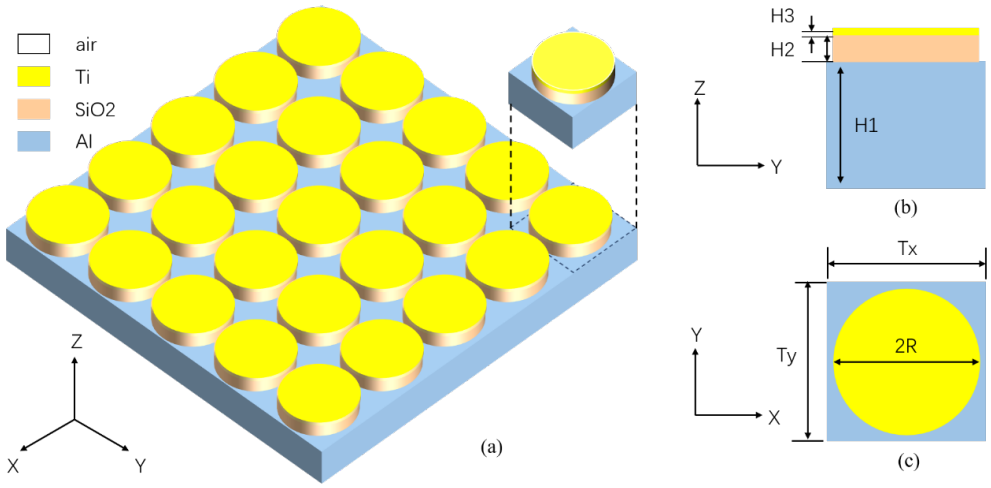

Figure 1: (a) Illustrates the cell structure, (b)Side view of single struct, (c)the top view of single struct

A full-field simulation of the proposed absorber was conducted using the finite difference time domain (FDTD) method [9], as illustrated in Figure 1(c). The absorber was modeled as a periodic structure in the X-Y plane and a perfect matched layer (PML) condition in the Z direction which exhibited absorption of reflected light and transmitted light. To expand the bandwidth as much as possible, this paper first optimizes the system parameters, and the values are as follows: H1=200nm, H2=85nm, H3=20nm, R=115nm, and Tx=Ty=250nm. As demonstrated in Figure 2(a), the absorption wavelength ranges from 300nm to 1200nm. This is consistent with the relationship between reflectance and absorbance as predicted by S-parameter theory [10,11]. Furthermore, Figure 2(b) illustrates the absorbance contributions of the various layers of the absorber. It can be observed that Ti has the primary contribution to the absorbance, while SiO_2 has a slight compensating effect in the violet wavelength band. This situation means that the wave impedance of SiO_2 is approximately equal to the vacuum wave impedance, resulting in a broadband absorber.

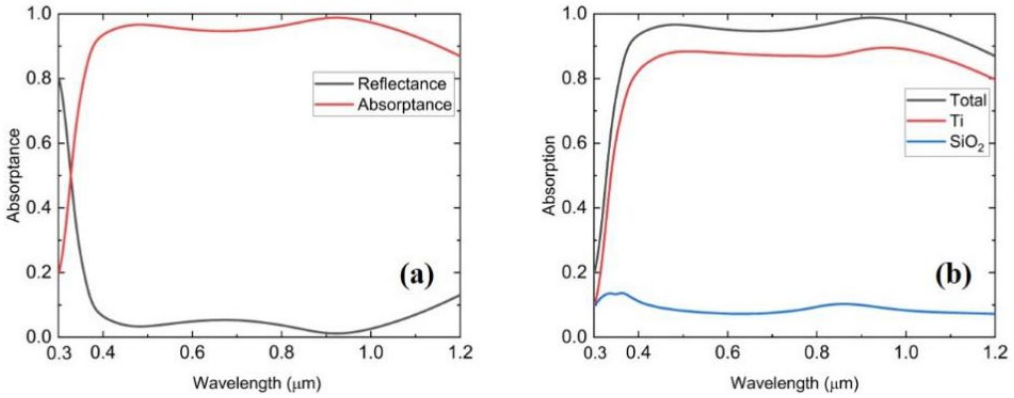

(a)Absorption spectra and Reflectance spectra of metamaterial absorber (Left)
(b) Absorbance contributions of different materials (Right)

Figure 2: Absorption diagram of the metamaterial absorber

ISSN 2616-5880 Vol. 5, Issue 3: 79-84, DOI: 10.25236/AJMC.2024.050312

3. Performance analysis

3.1 Field distribution at the positive incidence of light

For the sake of revealing the physical mechanism of the proposed metamaterial absorber, the distributions of current density, electric field, and magnetic field at various resonant wavelengths for the normal incidence of TE-polarized light are simulated. The side views of the three are obtained in Figures 3 to 5.

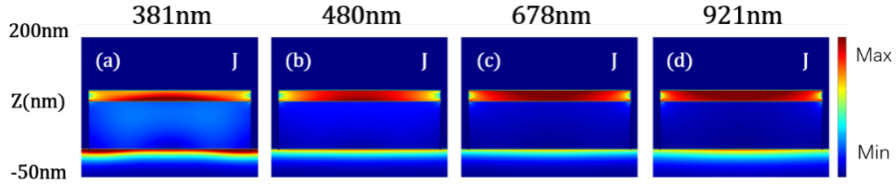

Figure 3: Current density distribution of metamaterial absorber

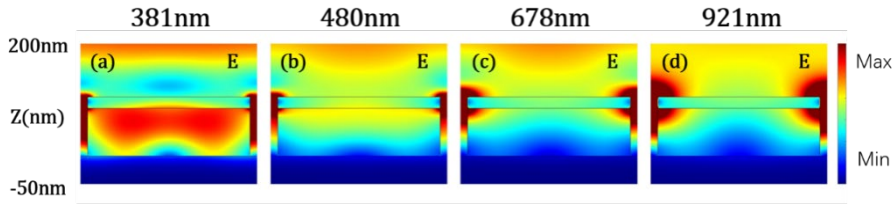

Figure 4: Electric field distribution of metamaterial absorber

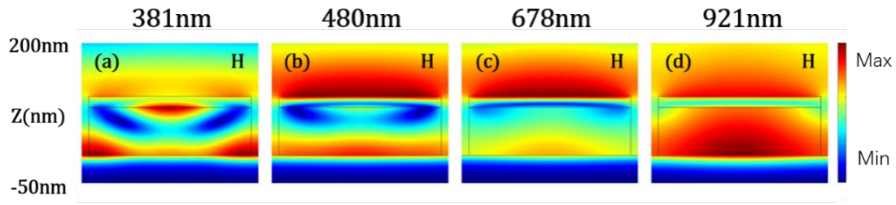

Figure 5: Magnetic field distribution of metamaterial absorber

As illustrated in Figure 3, the current distribution is predominantly concentrated at the top of the Ti and Al layers. The combination of them results in broadband absorption. As displayed in Figure 4, the distribution of the electric and magnetic fields reveals the excitation of surface plasmon polaritons (SPP) within the metamaterial structure. The coupling of light into the air gap and resonance within the SiO2 layer results in the generation of SPP, which subsequently undergoes absorption. In Figure 5, it can be seen that the magnetic field is markedly confined within the gap region situated beneath the nano-cube. The system exhibits resonance at 381 nm within the SiO2 disk and Al layer. At 921 nm, the magnetic field is predominantly confined between the Ti layer and the Al layer, undergoing Fabry–Pérot polaritons(FP) resonance with the intermediate bands, which display a combination of the two resonances. The electric and magnetic field maps show that in the top metal layer, the electric and magnetic resonances can be excited simultaneously at the resonance frequency, resulting in almost perfect absorption of the incident light wave. The distribution of electromagnetic field and current density shows the combination of different resonances such as SPP, PSP, and FP.

3.2 Optimization of structure and selection of materials

Subsequent studies sought to ascertain the impact of various metallic materials on the absorption characteristics. As illustrated in Figure 6(a), the upper metal exerts a profound influence on the position of the absorption peak and the width of the absorption spectrum. Ni and Ti exhibit high absorbance and extensive absorption bands within the visible and near-infrared regions. Ni holds considerable promise within the infrared band, although it displays slightly inferior performance. In the current absorber configuration, the incorporation of Ti facilitates a harmonious integration of the FP and SPP resonances, while the absorption band between the peaks exhibits a notable degree of absorbance. This is attributed to the material's relatively low-quality factor (Q-factor) [12], which ensures a stable absorbance across the

ISSN 2616-5880 Vol. 5, Issue 3: 79-84, DOI: 10.25236/AJMC.2024.050312

wavelength spectrum. As demonstrated in Figure 6(b), the bottom metals exert minimal influence on the absorption spectrum, as they have a negligible impact on the formation of the FP cavity. Their contribution is primarily manifested in the form of intrinsic absorption and transmittance, which is relatively low.

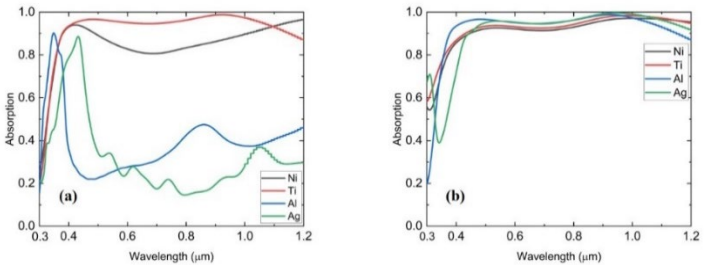

Figure 6: (a) Comparison of the absorption rate by replacing the top material (b) Comparison of absorption rate by replacing the bottom material

3.3 Analysis of oblique incidence and polarization

In order to completely measure the overall absorptivity of this absorber, this research paper analyzes the case of oblique incidence. It focuses on the absorptivity transformations in TE mode and TM mode. As shown in Figure 7, when the incidence angle is small (<40°), the absorber presents angular insensitivity to both polarizations. When the incidence angle continues to increase, the absorption rate decreases significantly. The absorption rate of the two modes decreases considerably in the long-wave band, and the absorption in the short-wave band shows a growing trend. The absorption peak in the center of the TE mode is red-shifted, and the change of the surface LSP resonance, and the peak wavelength of the TM mode is almost unchanged, which indicates that the TM mode is less affected by the LSP resonance. It indicates that the increase of the incident angle changes the LSP and PSP resonance conditions thus significantly decreasing the absorption rate.

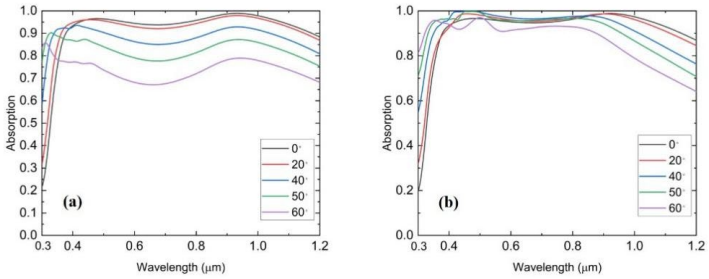

(a) TE mode oblique incidence, (b) TM mode oblique incidence absorptivity images

Figure 7: The effect of oblique incidence on absorption

It was observed that the absorptivity of the TM modes exhibited a greater decrease than that of the TE modes at large incidence angles. This phenomenon can be attributed to the process of polarization sensitivity, which is caused by material anisotropy and becomes increasingly significant with the increase of the oblique incidence angle. In particular, the present material demonstrates enhanced stability concerning oblique incidence angles of light, exhibiting a pronounced decline in absorptivity at elevated angles of oblique incidence and a notable distinction in the modes. Furthermore, the absorptivity remains largely unaltered below an incidence angle of 40°, exhibiting minimal polarization sensitivity.

ISSN 2616-5880 Vol. 5, Issue 3: 79-84, DOI: 10.25236/AJMC.2024.050312

4. Structural Comparison and Polarization Analysis

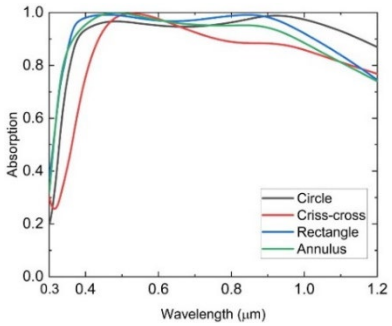

Figure 8: Absorption spectra of various structures

In order to further consider the practical use scenarios, this paper will proceed to discuss the shape of the absorber. The absorption spectra obtained by modifying the shape of the absorber to circular, cross, and square, while maintaining the thickness of the absorber constant, are illustrated in Figure 8. The findings indicate that the absorber structure exerts a relatively minor influence on the absorption spectra, which can be tailored to align with processing technology and the specific requirements of actual use scenarios. This suggests that the absorber may have a broader range of potential applications.

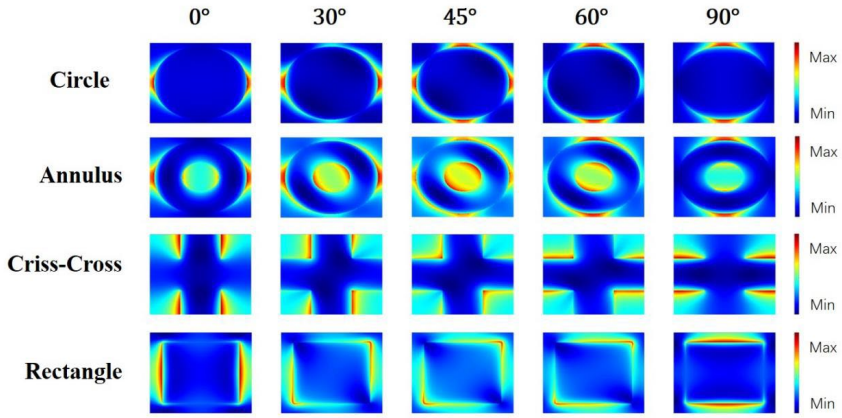

Figure 9: Electric field distribution on the surface of various structures

Furthermore, it is essential to examine the electric field maps for varying polarization states, as this will elucidate the nuances of the electric field distribution across different structural configurations. As shown in Figure 9, the electric field distribution on the surface of the absorber for different structures can be observed. The cross-shaped and square-shaped absorbers exhibit excellent capture of the electric field when polarized light is oriented at 0° and 90°, respectively. This indicates that these two structures are highly sensitive to the angle of polarization of the light. However, the electric field is unable to penetrate the absorber when the angle of polarization is 45°. This results in the light being less able to enter the resonance within the dielectric layer, which in turn leads to a reduction in the absorption rate. This indicates that these two structures are sensitive to the angle of polarization of light. In contrast, the polarized light at 45° on the surface of the circular and toroidal absorbers demonstrates a combination of 0° and 90°, indicative of substantial polarization orthogonality, and a concentrated distribution of electric field strengths, implying that it is coupled into the air spacer and enters the inner region of the absorber to complete the absorption process. This further suggests that it is polarization insensitive.

5. Conclusions

To sum up, this paper presents the design of a broadband visible absorber with MDM structure and an in-depth analysis of its absorption performance from multiple perspectives, including field distribution, structural and material characteristics, oblique incidence, and polarization. Moreover, the underlying mechanism of its metamaterial resonance absorption is elucidated. The designed metamaterial absorber exhibits an effective absorption band of 378-1152 nm, an operating bandwidth of 774 nm, an average absorption of 95.7%, and a peak absorption of 98.8%. Moreover, the metamaterial absorber displays angular insensitivity within a range of ±40°. The effective absorption band encompasses a wavelength

ISSN 2616-5880 Vol. 5, Issue 3: 79-84, DOI: 10.25236/AJMC.2024.050312

range of 378–1152 nm, with an operating bandwidth of 774 nm. The average absorption is 95.7%, while the peak absorption is 98.8%. The metamaterial absorber displays the angle of incidence and polarization insensitivity. Furthermore, it features a simple geometric configuration and a universal metallic composition. These properties demonstrate that the proposed metamaterial absorber is well-suited for a variety of applications, including optical communication, polarization detection, filtering, and sensing.

References

[1] Schurig D, Mock J J, Justice B J, et al. Metamaterial Electromagnetic Cloak at Microwave Frequencies [J]. Science, 2006, 314(5801):970-980.

[2] Valentine J, Zhang S, Zentgraf T, et al. Three-dimensional optical metamaterial with a negative refractive index[J]. Nature, 2008, 455(7211):376-379.

[3] Xu Cuilian, Meng Yueyu, Wang Jiafu, et al. Optically transparent hybrid metasurfaces for low infrared emission and wideband microwave absorption[J]. Acta Photonica Sinica, 2021, 50(4):0416001.

[4] Zhou W, Zhu Z H, Bai R R, et al. Broadband incident angle independent magnetic composite metamaterial absorber with C-band absorption [J].Optics and Laser Technology,2022,153:108031.

[5] Alkesh A, Mukul M, Ashutosh S. Wide incidence angle and polarization insensitive dual broadband metamaterial absorber based on concentric split and continuous rings resonator structure[J]. Materials Research Express, 2018, 5:115801.1-115801.10.

[6] Tran M C, Phuong T T H. Two-layered Dual-band Perfect Metamaterial Absorber at K band Frequency [J]. Advanced Electromagnetics, 2018, 7(2):25-27.

[7] Smith Endry. Homogenization of metamaterials by field averaging [J]. J Opt Soc Am B, 2006, 23(3):391-407

[8] Yu P, Besteiro LV, Wu J, Huang Y, Wang Y, Govorov AO, Wang Z. Metamaterial perfect absorber with unabated size-independent absorption. [J]. Opt Express, 2018, 26(16):20471-20480.

[9] Wallace JW, Jensen MA. Analysis of optical waveguide structures by use of a combined finite-difference/finite-difference time-domain method [J]. Opt Soc Am A Opt Image Sci Vis, 2002, 19(3):610-9.

[10] Smith D R, Schultz S. Determination of Effective Permittivity and Permeability of Metamaterials from Reflection and Transmission Coefficients [J]. Physical Review B, 2002, 65(19):195104.

[11] Smith D R, Vier D C, Koschny T, Soukoulis C M. Electromagnetic Parameter Retrieval from Inhomogeneous Metamaterials [J]. Physical Review. E, 2005, 71:036617.1-036617.11.

[12] Banerjee PP, Cook G, Evans DR. A q-parameter approach to analysis of propagation, focusing, and waveguiding of radially polarized Gaussian beams [J]. Opt Soc Am A Opt Image Sci Vis, 2009, 26(6):1366-74.